

# Probing Spindle Assembly Mechanisms with Monastrol, a Small Molecule Inhibitor of the Mitotic Kinesin, Eg5<sup>Ⓢ</sup>

Tarun M. Kapoor,\* Thomas U. Mayer,\* Margaret L. Coughlin,\* and Timothy J. Mitchison\*<sup>‡</sup>

\*Department of Cell Biology and <sup>‡</sup>Institute of Chemistry and Cell Biology, Harvard Medical School, Boston, Massachusetts 02115

**Abstract.** Monastrol, a cell-permeable small molecule inhibitor of the mitotic kinesin, Eg5, arrests cells in mitosis with monoastrol spindles. Here, we use monastrol to probe mitotic mechanisms. We find that monastrol does not inhibit progression through S and G2 phases of the cell cycle or centrosome duplication. The mitotic arrest due to monastrol is also rapidly reversible. Chromosomes in monastrol-treated cells frequently have both sister kinetochores attached to microtubules extending to the center of the monoaster (syntelic orientation). Mitotic arrest-deficient protein 2 (Mad2) localizes to a subset of kinetochores, suggesting the activation of the spindle assembly checkpoint in these cells. Mad2 localizes to some kinetochores that have attached microtubules in monastrol-treated cells, indicat-

ing that kinetochore microtubule attachment alone may not satisfy the spindle assembly checkpoint. Monastrol also inhibits bipolar spindle formation in *Xenopus* egg extracts. However, it does not prevent the targeting of Eg5 to the monoastrol spindles that form. Imaging bipolar spindles disassembling in the presence of monastrol allowed direct observations of outward directed forces in the spindle, orthogonal to the pole-to-pole axis. Monastrol is thus a useful tool to study mitotic processes, detection and correction of chromosome malorientation, and contributions of Eg5 to spindle assembly and maintenance.

Key words: monastrol • Eg5 • kinesin • MAD2 • kinetochore

## Introduction

During cell division, replicated DNA is segregated into two daughter cells by a bipolar spindle. Microtubules in the spindle form dynamic polymers along which chromosome movements are directed. These microtubules are nucleated by centrosomes and centrosome-associated proteins and are organized into bipolar arrays by motor proteins and microtubule-associated proteins (for reviews see Inoue and Salmon, 1995). Only after a functional spindle is assembled, with every chromosome correctly attached to microtubules, is sister chromatid segregation allowed by checkpoint proteins and cell division completed (for review see Rieder and Salmon, 1998).

Cell-permeable small molecules that rapidly activate or inactivate the function of their targets can be useful probes of dynamic cellular processes (Mitchison, 1994). For example, the small molecule colchicine led to the discovery of tubulin (Borisy and Taylor, 1967; Shelanski and Taylor,

1967) and has subsequently been used to probe the role of tubulin polymerization in dividing cells (Inoue and Salmon, 1995). Nocodazole, colcemid, and taxol also target tubulin and have been used to perturb microtubule dynamics in living cells. Studies with these small molecules have provided insights into the mechanisms that monitor cell cycle progression (Rieder and Palazzo, 1992; Waters et al., 1998). However, cell-permeable small molecules that target components of mitotic spindles other than tubulin were not known until recently.

We reported the discovery of monastrol, the first known cell-permeable small molecule inhibitor of the mitotic machinery that does not target tubulin (Mayer et al., 1999). Monastrol arrests cells in mitosis with monoastrol spindles comprised of a radial array of microtubules surrounded by a ring of chromosomes. We showed that monastrol does not affect microtubules in interphase cells or microtubule polymerization in vitro. Monastrol also does not perturb microtubule-dependent lysosome and Golgi apparatus distribution or chromosome dynamics in cells. The target of monastrol is likely to be the mitotic kinesin, Eg5. This motor protein is the vertebrate member of an evolutionarily conserved family of plus end-directed, bipolar kinesins,

<sup>Ⓢ</sup>The online version of this article contains supplemental material.

Address correspondence to Tarun M. Kapoor, Department of Cell Biology, Harvard Medical School, 240 Longwood Ave., Boston, MA 02115. Tel.: (617) 432-3728. Fax: (617) 432-3702. E-mail: tarun\_kapoor@hms.harvard.edu

whose founding member is the product of the bimC gene in *Aspergillus nidulans* (Enos and Morris, 1990). Mutations in genes encoding BimC family members in insect and fungal cells (Hagan and Yanagida, 1992; Hoyt et al., 1992; Roof et al., 1992; Heck et al., 1993), and inhibition of Eg5 with antibodies in human cells and in *Xenopus* egg extracts (Sawin et al., 1992; Blangy et al., 1995) have demonstrated the requirement of this kinesin in bipolar spindle formation.

Like antimicrotubule drugs, monastrol arrests cells in mitosis. Antimicrotubule drugs are thought to arrest cells by activating the spindle assembly checkpoint, a surveillance mechanism in cells that ensures the high fidelity of chromosome transmission. Genetic mutations that allowed yeast cells to progress through mitosis in the presence of small molecule inhibitors of microtubule polymerization led to the discovery of the mitotic arrest-deficient (*MAD*)<sup>1</sup> (Li and Murray, 1991) and budding uninhibited by benzimidazole (*BUB*) (Hoyt et al., 1991) genes. The products of these genes are part of the spindle assembly checkpoint pathway. More recently, the homologues of these yeast proteins have also been identified in vertebrates (Chen et al., 1996; Li and Benezra, 1996; Taylor and McKeon, 1997). It has been proposed that correct microtubule attachment at kinetochores, polynucleotide-polypeptide complexes on each sister chromatid, regulates the kinetochore association of checkpoint proteins and thereby contributes to checkpoint activation (Waters et al., 1998). However, checkpoint activation has not been examined with small molecules that do not perturb microtubule polymerization. A monoastrol spindle in which the microtubule organization is perturbed, rather than microtubule dynamics or nucleation, provides a distinct circumstance to unravel mechanisms that activate the spindle assembly checkpoint.

The assembly and maintenance of the bipolar spindle depends on force-generating motor proteins. Systematic deletion of kinesin genes in *Saccharomyces cerevisiae* has provided clear evidence for a balance of kinesin-dependent activities along the pole-to-pole axis in bipolar spindles. "Sliding filament" models have been proposed where motor protein-dependent cross-links arrange microtubules in bundles along which opposing forces can be applied (for review see Hildebrandt and Hoyt, 2000). Consistent with these models, yeast are viable in the presence of only two of six kinesins, Cin8p (an Eg5 homologue) and Kar3p or Kip3p, demonstrating possibly the simplest manifestation of a functional spindle (Cottingham et al., 1999) and a central role for Cin8 in establishing bipolar spindles (Saunders and Hoyt, 1992). More recently, analogous models have also been proposed for bipolar spindle formation and maintenance in *Drosophila* embryos (Sharp et al., 1999). The Eg5 homologue, Klp61F, has been proposed to oppose forces due to dynein and the Kin C kinesin, Ncd, allowing the maintenance of a constant pole-to-pole distance. However, these models do not consider forces perpendicular to the pole-to-pole vector in the spindle, the underlying microtubule dynamics, or the role of polewards

<sup>1</sup>Abbreviations used in this paper: CSF, cytotstatic factor; DIC, differential interference contrast; *MAD*, mitotic arrest-deficient; NuMA, nuclear/mitotic apparatus protein.

microtubule flux (Mitchison, 1989; Sawin and Mitchison, 1991). The contribution of kinesin-dependent forces to the lateral organization of chromosomes and microtubules in the spindle midzone has also not been explored.

In this report, we first evaluate the usefulness of monastrol as an agent to specifically and reversibly arrest cells in mitosis. We then use monastrol to probe two aspects of spindle assembly, mechanisms by which kinetochores signal to the spindle checkpoint pathway, and the forces that generate and maintain spindle bipolarity. In both cases, monastrol has revealed unexpected mechanistic insights.

## Materials and Methods

### Antibodies and Reagents

mAbs against  $\alpha$ -tubulin (DM1 $\alpha$ ; Sigma-Aldrich) were used at a 1:500 dilution. Human CREST (calcinosis, Raynaud's phenomenon, esophageal dysmotility, sclerodactyly, telangiectasia) serum, pAbs directed against MAD protein 2 (Mad2), and pericentrin were obtained as a gift from F. McKeon (Harvard Medical School, Boston, MA), E.D. Salmon (University of North Carolina, Chapel Hill, NC), and Y. Zheng (Carnegie Institute of Washington, Washington, DC), respectively. For immunofluorescence, the Mad2 and pericentrin antibodies were diluted 1:100 and 1:2,000, respectively. Human CREST serum was used at a 1:1,000 dilution. Anti-nuclear/mitotic apparatus protein (NuMA) antibodies were a gift from D.A. Compton (Dartmouth College, Dartmouth, NH) and C.E. Walczak (Indiana University, Bloomington, IN), and anti-Eg5 antibodies have been described previously (Walczak et al., 1998; Mountain et al., 1999). These antibodies were used at 1  $\mu$ g/ml. FITC- and Texas red-conjugated secondary antibodies (donkey) (Jackson ImmunoResearch Laboratories) were used at 15  $\mu$ g/ml. Monastrol was synthesized and purified using published methods (Mayer et al., 1999).

### Cell Culture

BS-C-1 (monkey epithelial kidney) and Ptk2 (rat kangaroo) cells were cultured in DMEM high glucose medium, supplemented with 10%FCS and 100 U/ml penicillin and streptomycin. The cells were maintained at 37°C and 5% CO<sub>2</sub>. For the double thymidine arrest, exponentially growing BS-C-1 cells were cultured for 16 h in normal growth medium containing 2 mM thymidine (Sigma-Aldrich). After this, the cells were released into normal growth medium supplemented with 24  $\mu$ M deoxycytidine (Sigma-Aldrich) for 9 h. The second thymidine block was imposed for 16 h during which the cells were maintained in serum-free medium containing 2 mM thymidine. Finally, the cells were released into normal growth medium containing 24  $\mu$ M deoxycytidine to which was added either 100  $\mu$ M monastrol or 0.1% DMSO. To assess the reversibility of the effect of monastrol and nocodazole treatment, BS-C-1 cells plated on coverslips were treated for 4 h in normal growth medium containing either 2  $\mu$ M nocodazole or 100  $\mu$ M monastrol and then released into normal medium. At the different time points, coverslips were processed for immunofluorescence and the cells in interphase or mitosis were counted and categorized.

### Electron Microscopy

To examine systematically the kinetochore-microtubule attachment on individual chromosomes, we used two different fixation conditions. In both cases, Ptk2 cells were cultured on poly-L-lysine-coated ACLAR coverslips (Ted Pella, Inc.). Condition 1 samples were permeabilized in buffer A (100 mM Pipes, pH 6.8, 1 mM MgCl<sub>2</sub>, 5 mM EGTA, and 0.1% Triton X-100) for 30 s at room temperature, then fixed with 1% glutaraldehyde in buffer A for 30 min followed by two rinses in buffer A and three rinses in 0.1 M cacodylate, pH 7.0. Condition 2 samples were permeabilized in buffer B (80 mM Pipes, pH 6.8, 1 mM MgCl<sub>2</sub>, 5 mM EGTA) with 0.1% Triton X-100 and 10  $\mu$ M Taxol for 3 min at 37°C, then fixed in 1% glutaraldehyde in buffer B with 10  $\mu$ M Taxol for 30 min at 37°C followed by two rinses in buffer B and three rinses in 0.1 M cacodylate, pH 7.0. Electron micrographs of samples prepared with condition 1 are shown in Fig. 4, A, D, and E; condition 2 was used for samples shown in Fig. 4, B and C.

Samples processed using condition 1 or 2 were postfixed in 1% osmium, 0.8% K<sub>3</sub>Fe(CN)<sub>6</sub> in 0.1 M cacodylate for 15 min, then rinsed two

times in 0.1 M cacodylate and three times in water before staining overnight in 1% aqueous uranyl acetate. They were dehydrated in a graded ethanol series and embedded in Epon araldite. Cells of specific phenotypes were identified, imaged with differential interference contrast (DIC) light microscopy, excised, and remounted. Serial sections of 65 or 85 nm were cut on a Reichert Ultracut S microtome, picked up on formvar-coated slot grids, stained with 2% uranyl acetate in 50% methanol and lead citrate, then viewed and imaged on a JEOL 1200 EX electron microscope.

### **Preparation and Imaging of Spindles in *Xenopus* Egg Extracts**

Cytoplasmic extracts of unfertilized *Xenopus* eggs arrested in metaphase of meiosis II by cytostatic factor (CSF) activity were prepared fresh as described (Desai et al., 1999). Spindles were assembled in extracts with sperm nuclei cycled through interphase. Tetramethyl rhodamine-labeled calf brain tubulin (0.2 mg/ml) (Hyman et al., 1991) and Hoechst 33342 (100 ng/ml; Sigma-Aldrich) were added to the assembly reactions to visualize the microtubules and chromatin, respectively. Monastrol was typically prepared as a 50× stock of the desired final concentration in sperm dilution buffer (10 mM HEPES, pH 7.7, 1 mM MgCl<sub>2</sub>, 100 mM KCl, and 10 μg/ml cytochalasin B). At the appropriate time in the assembly reaction, monastrol was added directly to the extract and mixed thoroughly but gently. Real time images were acquired on a Nikon TE-300 microscope. For disassembly reactions in the presence of monastrol, 4 μl of extract was placed under a coverslip separated from a slide by two strips of double stick tape. Very thin sample preparations did not disassemble at rates observed for reactions in Eppendorf tubes. 1 μl samples were removed from reactions at different times and fixed for quantitation (see Desai et al., 1999).

### **Immunofluorescence**

Cells cultured on glass coverslips were permeabilized and fixed for 10 min in a buffer containing 100 mM Pipes (pH 6.8), 10 mM EGTA, 1 mM MgCl<sub>2</sub>, 0.2% Triton X-100, and 4% formaldehyde (Sigma-Aldrich). For the calcium treatment, samples were permeabilized for 90 s in a buffer containing 100 mM Pipes (pH 6.8), 1 mM MgCl<sub>2</sub>, 0.1 mM CaCl<sub>2</sub>, and 0.1% Triton X-100 and then fixed for 10 min in the same buffer supplemented with 4% formaldehyde. Samples for immunofluorescence from *Xenopus* egg extracts were prepared by diluting spindle assembly reactions and spinning them onto coverslips as described (Desai et al., 1999). After three washes with TBS containing 0.1% Triton X-100 (TBST), nonspecific antibody binding was blocked for 10 min with 2% BSA in TBST. Incubations with primary antibodies were carried out overnight at 4°C in TBST. Bound antibody was visualized by incubation with fluorescence-conjugated secondary antibody for 1 h. After three washes with TBST containing 10 μg/ml Hoechst 33342, the coverslips were mounted in 80% glycerol, 20 mM Tris (pH 8.8), and 10 mg/ml *p*-phenylenediamine (Free Base; Sigma-Aldrich). Immunostained samples were imaged on an Olympus IX70 inverted microscope, and series of optical sections were collected by wide field deconvolution 3D microscopy (Agard et al., 1989) using a 60× 1.4 numerical aperture lens. Images shown are maximum intensity projections of deconvolved stacks.

### **Online Supplemental Material**

Online supplemental material includes a Quicktime® video corresponding to Fig. 10 and data showing that monastrol does not inhibit the microtubule binding of recombinant Eg5 in vitro. See <http://www.jcb.org/cgi/content/full/150/5/975/DC1>.

## **Results**

### **Monastrol Causes a Specific and Reversible Cell Cycle Block**

To test the utility of monastrol as a reagent for mitosis research, we examined its effects on phases of the cell cycle other than mitosis. The percentage of cells with monoastrol spindles that accumulate in an asynchronous population of BS-C-1 (monkey epithelial kidney) cells treated

with monastrol for 4 h increases with drug concentration (Fig. 1, A and C, MA). We used 100 μM as a saturating dose for further experiments. To test whether monastrol delays the progression of cells through S and G<sub>2</sub> phases or entry into the M phase of the cell cycle, we synchronized BS-C-1 cells using a double thymidine block and released them into 100 μM monastrol. Monastrol-treated cells enter mitosis with kinetics identical to untreated cells, consistent with the small molecule having a mitosis-specific effect (Fig. 1 B). In monastrol, cells accumulate in mitosis with monoastrol spindles and the mitotic arrest is persistent for at least 12 h (data not shown).

To test the reversibility of the mitotic arrest due to monastrol, we fixed BS-C-1 cells at different times after removal of monastrol from the cell culture media. The tubulin and chromatin organization in the cells was examined and the observed structures were divided into the four categories shown in Fig. 1 C. Within 15 min after removal of monastrol, almost all monoasters in cells were replaced by bipolar spindles. Cells with normal bipolar spindles with chromosomes aligned at metaphase plates predominated at 30 min after release and by 60 min, most cells were observed in late anaphase or cytokinesis (Fig. 1 D).

We compared the reversibility of the mitotic arrest due to monastrol with that due to nocodazole (Fig. 1 E). Nocodazole depolymerizes microtubules in cells at all stages of the cell cycle, but cells arrest in metaphase with condensed chromatin and no mitotic spindle (Fig. 1 C, NoS). On removing nocodazole from the cell culture media, microtubules polymerize and a new spindle is assembled. Even 30 min after the release of the arrest, most of the cells have spindles without aligned chromosomes. Anaphase in these cells is also delayed compared with cells released from a monastrol arrest.

Using phase-contrast microscopy, we have imaged live BS-C-1 cells released from a monastrol arrest (data not shown). The monoaster in every cell imaged formed a bipolar spindle and the cell completed cytokinesis with normal kinetics; the rates in these experiments correlated well with the data in Fig. 1 D. Compared with nocodazole-treated cells, which presumably need to polymerize a new microtubule array and then build a bipolar spindle, removing monastrol from treated cells allows the rapid generation of spindle bipolarity since all components of the spindle appear to be present but incorrectly organized. Thus, using monastrol to arrest cells may provide a more rapidly reversible block for mitotic research in general.

### **Monastrol Inhibits Centrosome Separation Not Duplication**

In principle, monoastrol spindles might be generated by inhibition of centrosome duplication (Sluder et al., 1989; Winey et al., 1991), inhibition of centrosome separation (Hoyt et al., 1992; Sawin et al., 1992; Heck et al., 1993), or normal duplication and separation followed by spindle collapse (Sharp et al., 1999). To examine the effect of monastrol on the centrosome cycle, we determined the number of centrosomes in monastrol-treated cells using serial section electron microscopy. Fig. 2 A shows a micrograph of a monastrol-treated Ptk2 (rat kangaroo kidney epithelium) cell after it has been processed for thin section

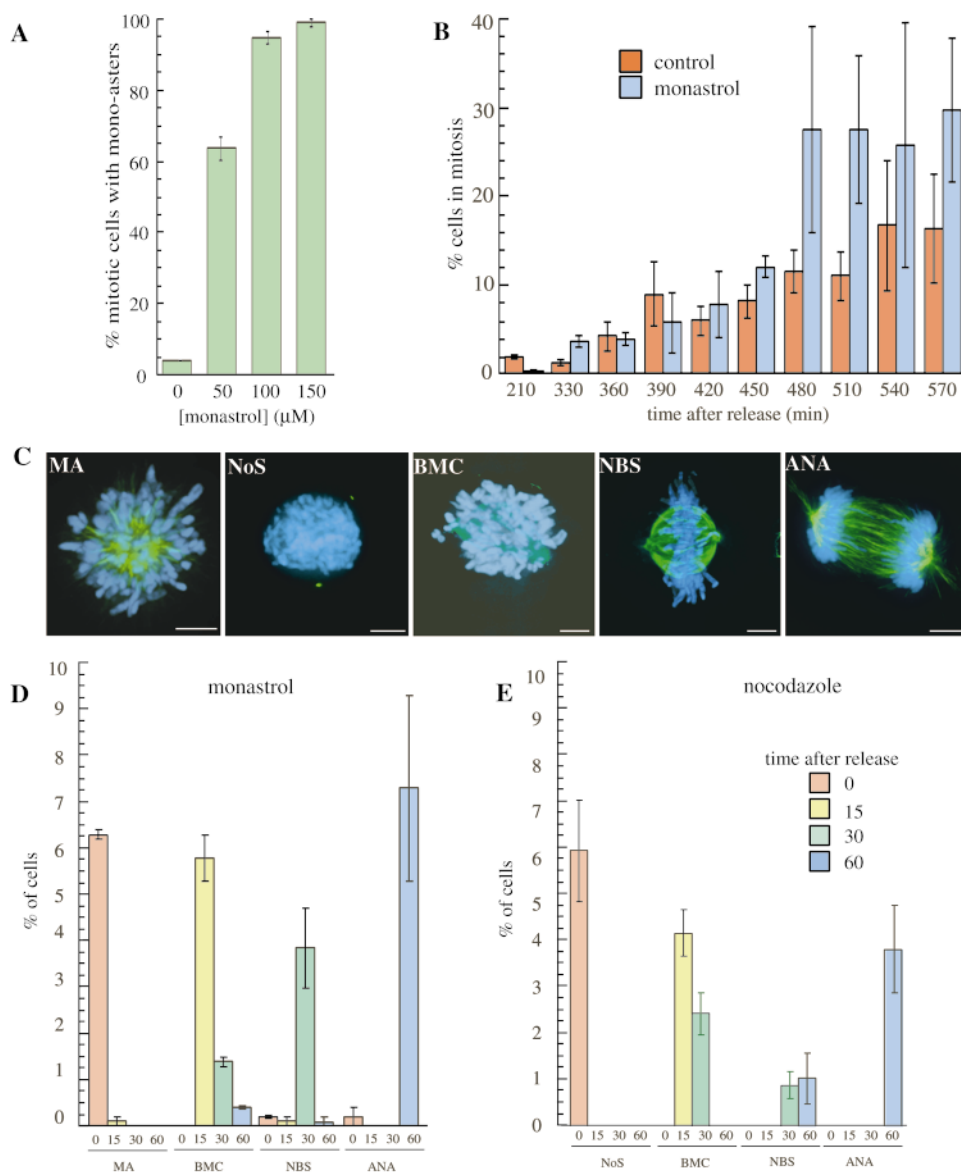


**Figure 1.** Characterization of the mitotic arrest due to monastrol. (A) Percentage of monoastrol spindles in mitotic BS-C-1 cells treated with monastrol for 4 h. (B) Monastrol does not delay the entry of synchronized BS-C-1 cells into mitosis. 100  $\mu$ M monastrol or DMSO solvent was added to cells at the time of releasing the second thymidine block, and the percentage of cells in M phase at the indicated times after the release was determined by staining fixed cells for chromatin and microtubules. (C) Cytology of cells before and after removal of monastrol and nocodazole. Immunofluorescence staining of  $\alpha$ -tubulin (green) and chromatin (blue) in BS-C-1 cells was used to examine cellular structures. Representative structures, including monoastrol spindles (MA) in monastrol-treated cells, the no spindles (NoS) phenotype seen in cells treated with nocodazole, misaligned chromosomes on bipolar microtubule arrays (BMC), chromosomes aligned at the metaphase plate in bipolar spindle (NBS), and anaphase (ANA) structures in cells exiting mitosis are shown. (D) Reversibility of the mitotic arrest due to monastrol. The percentage of cells in four structural categories, MA, BMC, NBS, and ANA, was determined at fixed intervals after washout of saturating concentrations of monastrol (100  $\mu$ M) from the cell culture media. (E) Histogram show the percentage

of cells with different structure types (NoS, BMS, NBS, and ANA) that form 15, 30, and 60 min after the release of the mitotic arrest due to nocodazole (2  $\mu$ M), a microtubule depolymeriser. Data from two independent experiments are shown for A, B, D, and E; for each entry, >200 cells were counted, and the SE is indicated. Bars: (C) 5  $\mu$ m.

electron microscopy. The higher magnification images show four centrioles, corresponding to two replicated centrosomes, at the center of the monoaster. The centrosomes in the cell shown are separated by 1.0  $\mu$ m, and the two centrioles within each centrosome are found in adjacent sections. Similar results were found for five other cells examined by electron microscopy. Untreated cells have two centrosomes, each with two centrioles, at opposite ends of a bipolar spindle (Fig. 2 B). Thus, monastrol does not affect the number of centrosomes in cells but inhibits their separation. The structure and size of the centrioles in monastrol-treated and untreated cells are similar, indicating that monastrol does not interfere with centriole replication or centrosome organization.

To quantitate the separation of the centrosomes in monastrol-treated cells, we immunolocalized pericentrin, a marker for centrosomes (Khodjakov et al., 2000), in mi-

totic Ptk2 cells treated with different concentrations of monastrol. Fig. 2 C shows two dots of pericentrin in a monastrol-treated cell, indicating that the replicated centrosomes are only slightly separated. In control cells, the average separation of the centrosomes at metaphase was 18.7 ( $\pm$  1.0)  $\mu$ m. These results are quantitated in Fig. 2 D. Greater than 50% reduction in centrosome separation is observed at 50  $\mu$ M monastrol. At 100  $\mu$ M monastrol, the centrosome separation in inhibited mitotic cells is similar to that in untreated interphase cells with replicated centrosomes (data not shown). These observations indicate that monastrol inhibits the activities driving centrosome separation in cells and are consistent with genetic data on Eg5 inhibition (Hagan and Yanagida, 1992; Hoyt et al., 1992; Heck et al., 1993). The influence of these unseparated centrosomes on microtubule organization results in monoastrol spindles.

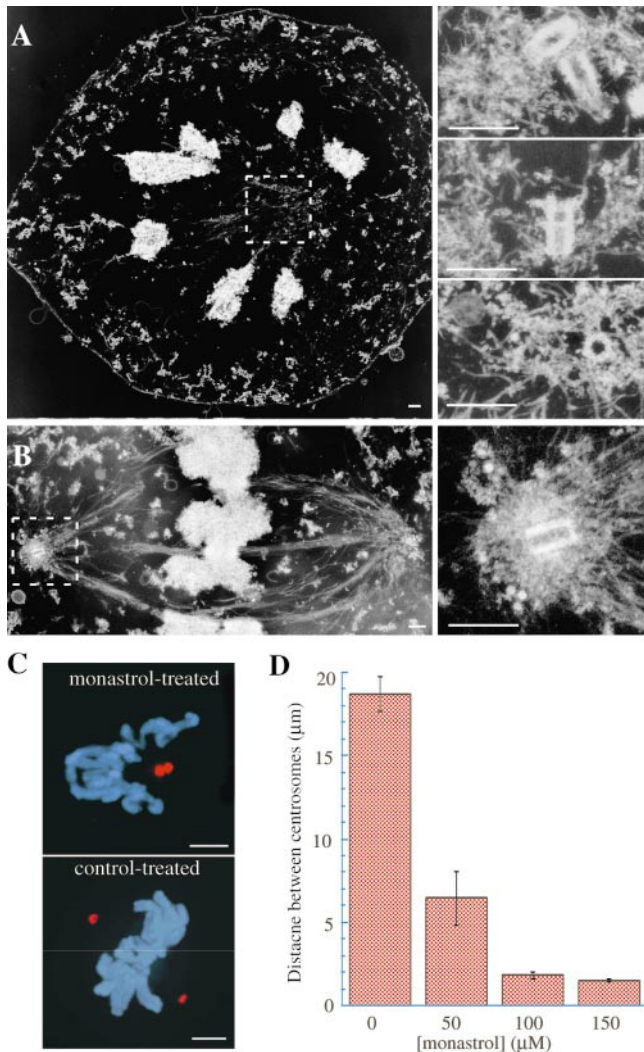


**Figure 2.** Monastrol does not inhibit centrosome duplication but inhibits centrosome separation. (A) A representative electron micrograph of a Ptk2 cell treated with 50  $\mu\text{M}$  monastrol for 4 h. The monoastral spindle has chromosomes arranged in a ring at the center of which are two centrosomes. Higher magnification electron micrographs are shown in three insets. Two centrioles corresponding to one centrosome are found in a single section, and the two centrioles from the other centrosome are in two adjacent sections. (B) Control cell. The inset shows a high magnification image of one of the four centrioles observed in this cell. Centrioles in untreated cells have sizes and morphologies identical to that of centrioles in monastrol-treated cells. (C) Immunolocalization of a centrosomal marker, pericentrin (red), in Ptk2 cells treated with 50  $\mu\text{M}$  monastrol, shows two dots at the center of the cell. The bottom panel shows chromatin (blue) at the metaphase plate in a control cell with a bipolar spindle. The dots of pericentrin staining on opposite sides of chromosomes are separated by 18  $\mu\text{m}$ . (D) Centrosome separation in mitotic Ptk2 cells treated with different concentrations of monastrol. The distance between the dots of pericentrin staining in light micrographs was measured. Averages of distances measured for 15 cells at each monastrol concentration are shown ( $\pm\text{SE}$ ). Metaphase cells were chosen in untreated cells (zero monastrol). Bars: (A and B) 0.5  $\mu\text{m}$ ; (C) 5  $\mu\text{m}$ .

Live images of BS-C-1 cells showed that interphase cells entering mitosis in the presence of 100  $\mu\text{M}$  monastrol do not form bipolar spindles (data not shown). Instead, they proceed directly to the monoastral state. Addition of monastrol to cells that have already established a bipolar spindle did not result in spindle collapse, and anaphase was not inhibited in these cells.

### ***Immunostaining Kinetochores in Monastrol-treated Cells Reveals Syntelic Oriented Chromosomes Attached to Microtubules***

We next examined the microtubule attachment and the orientation of sister kinetochores on chromosomes in monastrol-treated cells. In brief, treating mitotic cells with calcium during permeabilization and before fixation destabilizes nonkinetochore microtubules, leaving behind mainly kinetochore microtubules (Mitchison et al., 1986). Fig. 3 shows a monastrol-arrested Ptk2 cell cleared of its nonkinetochore microtubules, stained for kinetochores and tubulin. Stable kinetochore microtubules are seen in the monoastral structures that result from monastrol treatment. Although the molecular basis of the stability of the kinetochore microtubules to calcium treatment is not known, we find that kinetochore microtubules are stabilized to similar extents in monastrol-treated and untreated cells. Each condensed chromosome in this Ptk2 cell has two sister kinetochores, as expected. The J and V shapes of the chromosomes are indicative of their dynamic attachment to the radial array of microtubules in the monoastral spindle. To our surprise, in most cases both kinetochores on sister chromatid pairs appeared to be attached to kinetochore microtubule bundles that extend to the center of the monoaster (see Table I). This orientation, termed syntelic orientation, is distinct from monotelic orientation, where one sister kinetochore is oriented to a spindle pole and the other oriented in the opposite direction, and amphitelic orientation, where two sister kinetochores are oriented to opposite poles in a bipolar spindle (Roos, 1976; Rieder, 1982). Monotelic and amphitelic orientations are typically observed in chromosomes in prometaphase and metaphase cells. Syntelic orientation has been observed for meiotic chromosomes (for reviews see Nicklas, 1971; Rieder, 1982). However, syntelic orientation for mitotic marsupial cells in culture has been documented as a rare event (Roos, 1973; Roos, 1976).

### ***Analysis of Kinetochore Orientation and Microtubule Attachment in Monastrol-treated Cells by Electron Microscopy***

Having observed syntelic oriented chromosomes with both sister kinetochores attached to microtubules in calcium-permeabilized, monastrol-treated cells, we used correlative light and electron microscopy to examine more carefully the kinetochore structure and microtubule attachment in these chromosomes. Fig. 4 A shows a DIC image of a mitotic Ptk2 cell treated with 50  $\mu\text{M}$  monastrol, embedded in plastic. We then used serial section electron microscopic analysis to determine the orientation and microtubule attachment for both sister kinetochores for as many chromosomes as possible, in this cell (summarized in Table II). The ultrastructure of each kinetochore for the chromo-



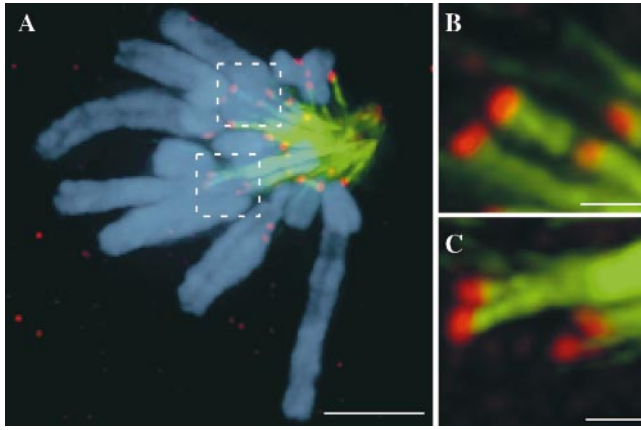


**Figure 3.** Calcium-stable kinetochore microtubules in monastrol-treated cells. Cultured Ptk2 cells were treated with 50  $\mu$ M monastrol for 4 h, permeabilized for 90 s in the presence of 0.1 mM calcium, then fixed and immunostained. Calcium treatment selectively removes nonkinetochore microtubules. Each chromosome (blue) has two kinetochores (red) that stain with CREST serum (A). In many cases, microtubule bundles (green) emanating from the pole attach to kinetochores. Several examples with both kinetochores of a sister pair attached to microtubules are observed. B and C show higher magnification micrographs for four pairs of kinetochores attached to microtubules. Bars: (A) 5  $\mu$ m; (B and C) 1  $\mu$ m.

somes numbered 1, 2, and 3 in the light micrograph of the cell is shown (Fig. 4 A). In each of these chromosomes, both kinetochores were attached to microtubules and were oriented in the same direction towards the center of the monoastral spindle, consistent with our immunofluorescence data (Fig. 3). The organization and ultrastructure of syntelic kinetochores observed in monastrol-treated cells are similar to previously documented structures that resulted from spontaneous mistakes (Roos, 1976; Rieder, 1982).

The orientation and attachment of chromosomes in other monastrol-treated Ptk2 cells are shown in Fig. 4, B–D. In Fig. 4, B and C, are other typical syntelic oriented chromosomes. Fig. 4 D shows an example of a monotelic chromosome (with only one kinetochore attached [k1] to microtubules and the other unattached [k2], and facing in the

**Table I.** Statistics for Kinetochore–Microtubule Attachment Observed by Light Microscopy, in Monastrol-treated Ptk2 Cells Fixed after Calcium Treatment

Cell	Chromosomes with both kinetochores attached to microtubules	Chromosomes with one kinetochore attached to microtubules	Chromosomes with no kinetochores attached to microtubules
1	10	4	0
2	10	3	0
3	10	3	0
4	8	4	0
5	11	2	0
Percent ( $\pm$ SD) chromosomes (14 total)	70 ( $\pm$ 8)%	23 ( $\pm$ 6)%	0 ( $\pm$ 0)%

**Table II.** Analysis of Chromosome Orientation and Kinetochore–Microtubule Attachment in Monastrol-treated Ptk2 Cells Analyzed by Serial Section Electron Microscopy

Cell	Chromosomes serially sectioned	Unambiguous syntelic oriented chromosomes	Unambiguous monotelic chromosomes	Unattached chromosomes
1	13	3 (6)	0	0
2	13	4 (7)	1 (1)	0
3	6	3 (6)	0	0

In parentheses is the number of kinetochores attached to microtubules for each type of chromosome orientation found in the cells.

opposite direction) in a monastrol-treated cell. Monotelic chromosomes were also observed but much less frequently than the syntelic oriented chromosomes, though there may be some bias in our ability to detect syntelic versus monotelic orientation, since kinetochores with no microtubules attached may escape detection by electron microscopy. Completely unattached chromosomes were not seen. Due to the shape of the cell and the limitations of thin section electron microscopy, we were unable to analyze every kinetochore for every chromosome in any one cell. We have been very conservative in categorizing kinetochores for individual chromosomes, and only chromosomes for which we unambiguously identified both kinetochores as distinct plates are listed in Table II. Our analysis indicates that at least 23% of the chromosomes had syntelic orientation with both kinetochores attached to microtubules. Less stringent interpretation of these electron micrographs and analyses of the images from light microscopy after calcium treatment (Table I) suggest that 70% of the chromosomes in monastrol-treated cells can have syntelic oriented sister kinetochores.

### **Mad2 Localizes to Microtubule-attached Kinetochores in Monastrol-arrested Cells**

To examine the mechanism of the mitotic arrest induced by monastrol, we asked whether monastrol inhibits mitosis by activating the spindle assembly checkpoint. In marsupial cells, the localization of Mad2 to kinetochores has been used as a marker for those kinetochores that have not satisfied the checkpoint (for review see Rieder and Salmon, 1998). Fig. 5 A shows Mad2 immunolocalized to all unattached kinetochores on condensed chromatin in an early prometaphase Ptk2 cell. Immunolocalization of Mad2 in a monastrol-treated cell is shown in Fig. 5 B. Strong Mad2 staining, at least equivalent to that on prometaphase kinetochores, colocalized with a subset of kinetochores. Further analysis showed that for most of the chromosomes in a monastrol-treated cell, Mad2 localized to one of the two sister kinetochores (see Table III). Typically, though not always, strong Mad2 staining was observed on the kinetochore further from the pole while its sister was almost completely devoid of Mad2 staining.

Previous studies using small molecules to perturb microtubule dynamics and polymerization have shown that the kinetochore localization of Mad2 is sensitive to microtubule attachment (Waters et al., 1998). Based on our analysis of the microtubule attachment of chromosomes (see Tables I and II), we expected as many as 70% of the chromosomes to have both kinetochores attached to microtu-

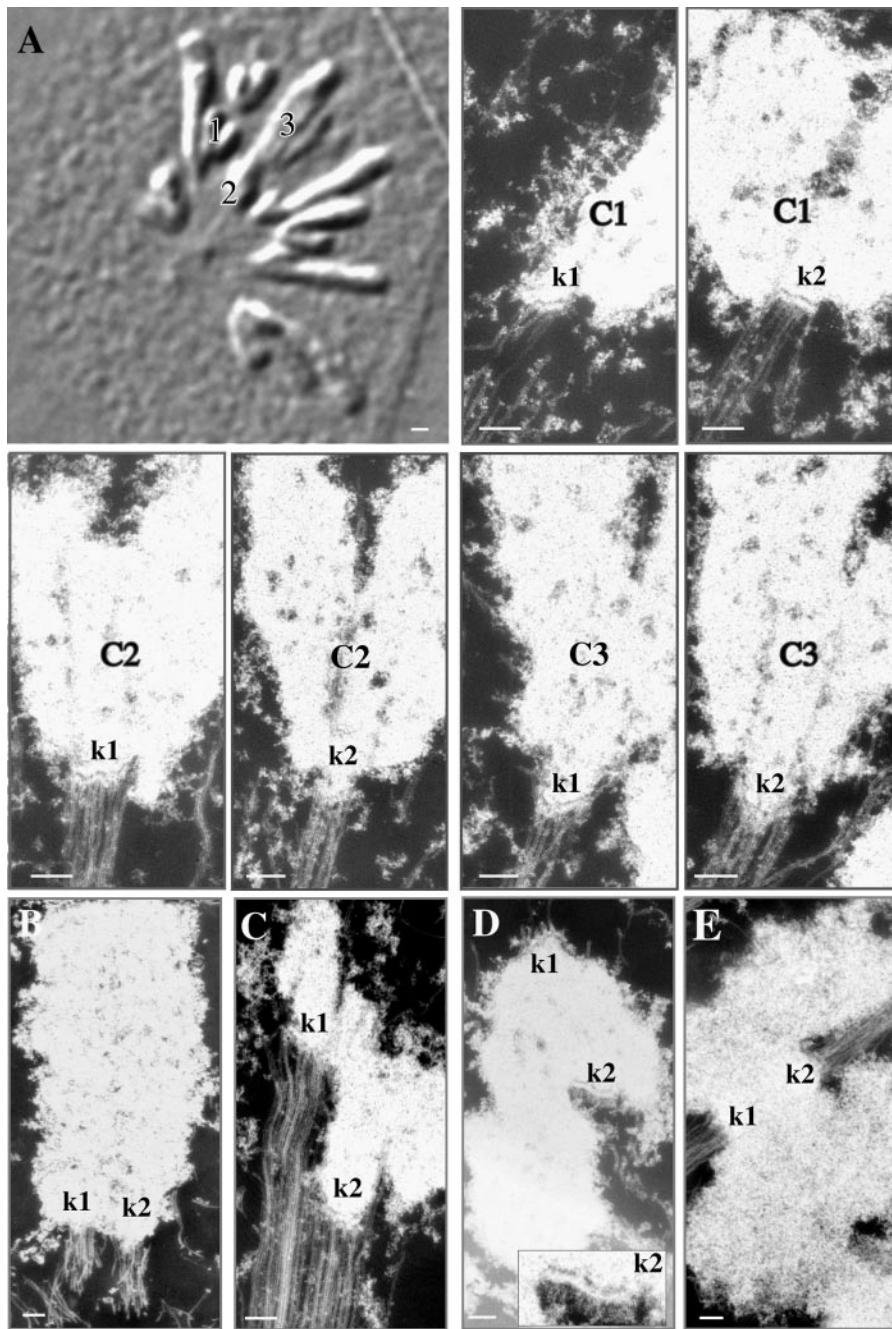


**Figure 4.** Chromosomes in monastrol-treated cells are attached to microtubules and can show syntelic orientation. (A) A DIC micrograph of a monastrol-treated cell that has been permeabilized, fixed, and embedded in plastic. Note the arrangement of the chromosomes in the monoaster. After this image was taken, the cell was serially sectioned and examined by electron microscopy. For three chromosomes, labeled 1, 2, and 3 in the DIC image, we show three pairs of electron micrographs, labeled C1, C2, and C3. Sister kinetochores for each chromosome are labeled (k1 and k2) and are found in different sections. Both kinetochores in a sister pair are attached to similar numbers of microtubules and have distinct outer plates. (B and C) A monastrol-treated cell permeabilized in the presence of 10  $\mu\text{M}$  taxol also has syntelic oriented chromosomes with several microtubules attached to each kinetochore. Even under these conditions, the two syntelic chromosome in this cell have both kinetochores oriented in the same section and each kinetochore is attached to several microtubules in the monoastrol spindle (see Table II for a complete analysis). (D) A monotelic chromosome from this cell is shown with one kinetochore (k1) oriented to the center of the monoaster and the other kinetochore (k2) oriented in the opposite direction. One kinetochore (k1) on this chromosome has attached microtubules in an adjacent section. The inset provides a 2.5-fold magnification of the unattached kinetochore labeled k2. (E) Ultrastructural analysis of a control, untreated cell shows bioriented kinetochores on either side of a chromosome attached to microtubules from opposite poles in the bipolar spindle. Bars: (A, DIC image) 1  $\mu\text{m}$ ; (A, electron micrographs, and B–E) 200 nm.

bules. However, on average, 85% of the chromosomes in a cell have Mad2 immunolocalized to one or both sister kinetochores on a chromosome (Table III). Based on this statistical analysis, we inferred that some kinetochores must be both Mad2 positive and also attached to microtubules. To examine this, we stained a monastrol-treated cell for chromatin, tubulin, kinetochores, and Mad2 after using calcium to selectively remove nonkinetochore microtubules (Fig. 6 A). The insets show two kinetochores (red) on two different chromosomes in the monoaster, attached to microtubules (green). Both these kinetochores stain for Mad2 (blue in the inset). For four cells, we examined the localization of Mad2 and the attachment of sister kinetochores to microtubules for every chromosome for which

we could unambiguously identify both sister kinetochores. Of the chromosomes that have syntelic orientation and have both kinetochores attached to microtubules (64%), 84% had at least one kinetochore positive for Mad2. This indicates that the localization of Mad2 cannot be sensitive only to microtubule attachment.

### ***Monastrol Inhibits Bipolar Spindle Assembly in *Xenopus* Egg Extracts***

To examine the roles of kinesin-dependent forces in bipolar spindle formation and maintenance, we used monastrol to inhibit Eg5 in *Xenopus* egg extracts. This cell-free extract system can assemble bipolar spindles in vitro and re-

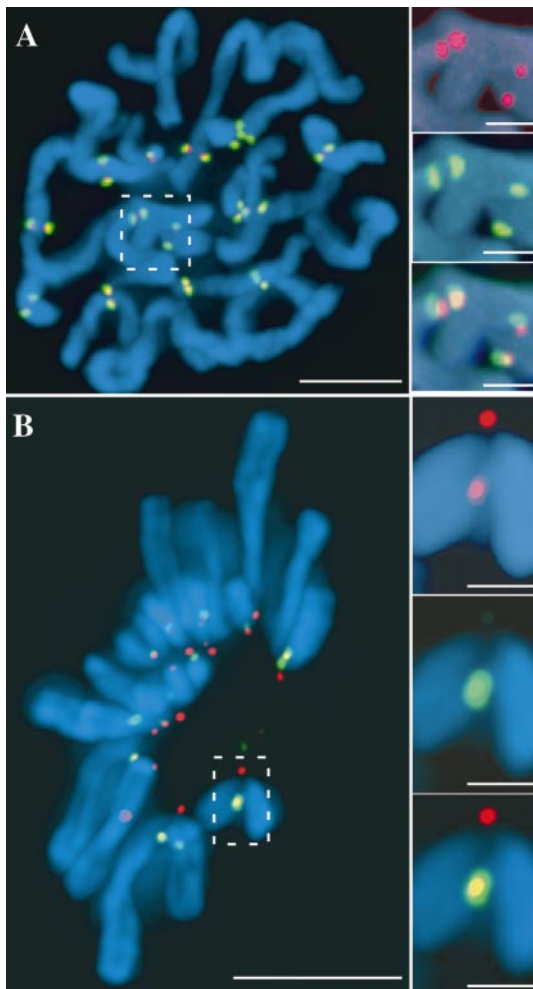


**Figure 5.** Monastrol activates the MAD-dependent spindle assembly checkpoint. Immunofluorescence staining was used to localize Mad2 (green) on chromosomes (blue) in fixed Ptk2 cells. Kinetochores are immunolabeled with CREST serum (red). (A) Condensed chromosomes in a prometaphase cell have two kinetochores, one on each replicated sister chromatid. The overlay and the insets show Mad2 localized to each kinetochore. (B) Ptk2 cells treated with 50  $\mu\text{M}$  monastrol show Mad2 localized to only one of the two kinetochores on sister chromatid. The insets show a chromosome with Mad2 localized to a kinetochore further from the center of the monoastral spindle: top, kinetochore alone; middle, Mad2 alone; bottom, overlay. Table III provides an analysis of the Mad2 staining for five monastrol-treated cells. Bars: (A and B) 5  $\mu\text{m}$ ; (A and B insets) 1  $\mu\text{m}$ .

capitulate several aspects of mitotic processes, making it a useful system to probe the function of spindle proteins, including Eg5 (Sawin et al., 1992; Walczak et al., 1998). First, we examined the effect of monastrol on bipolar spindle formation. Bipolar spindles were assembled in extracts where the sperm nuclei have been cycled through interphase to allow for chromosome and centrosome replication (Fig. 7) (Desai et al., 1999). Addition of monastrol at the time of CSF addition inhibited the formation of bipolar spindles in a dose-dependent manner. The  $\text{IC}_{50}$  (median inhibitory concentration) was 20  $\mu\text{M}$  and is similar to that observed for intact BS-C-1 cells. The morphological

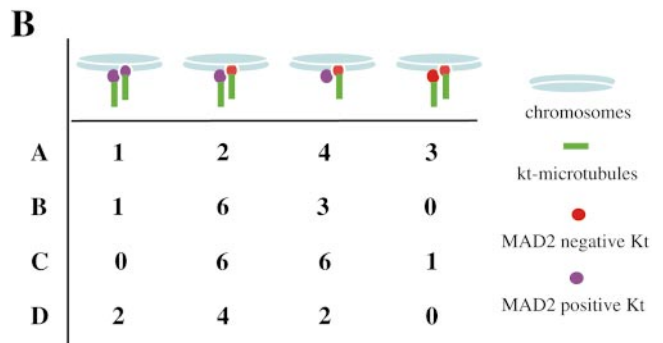
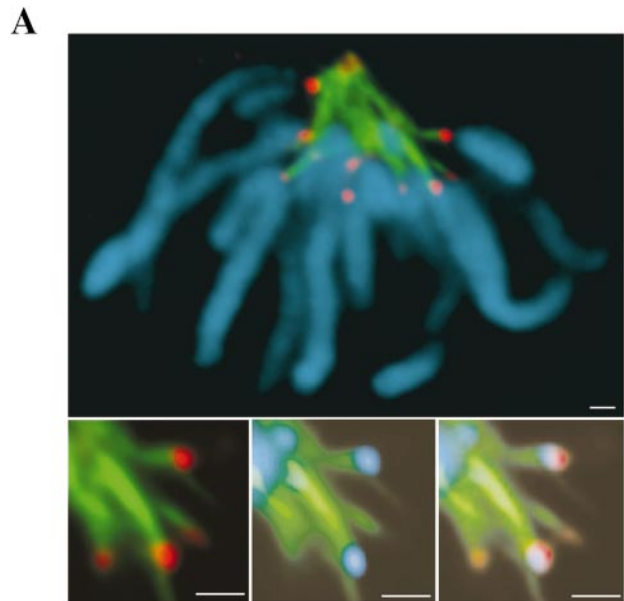


**Figure 6.** Mad2 localized to microtubule-attached kinetochores in monoastral spindles. (A) Monastrol (50  $\mu\text{M}$ ) treated Ptk2 cells permeabilized in the presence of 0.1 mM calcium before fixation were stained with Hoechst 33342, antitubulin (mouse), antikinetochore (human CREST serum), and anti-Mad2 (rabbit). A single optical section of a monoastral spindle is shown with DNA (blue), tubulin (green), and kinetochores (red). The insets show two kinetochores on two different chromosomes from the cell showing the tubulin (green), kinetochores (red) (left), tubulin and Mad2 (blue) center, and a three color overlay (right) indicating the presence of Mad2 on two microtubule-attached kinetochores. (B) Four quadruple stained cells were optically sectioned, and chromosomes in these cells were sorted into the following categories: those with both kinetochores attached to microtubules and both kinetochores Mad2 positive; those with both kinetochores attached to microtubules and only one kinetochore Mad2 positive; those with one kinetochore attached to microtubules and Mad2 negative, and the other kinetochore unattached and Mad2 positive; and those with both kinetochores attached to microtubules and both kinetochores Mad2 negative. Bars: 1  $\mu\text{m}$ .

effect of monastrol is similar to that seen for antibody inhibition of Eg5 in *Xenopus* egg extracts.

We next compared the localization of Eg5 in control bipolar spindles and monoastral spindles assembled in the presence of monastrol (Fig. 8). In untreated bipolar spindles, Eg5 is localized throughout the spindle with an enrichment at the poles (Fig. 8 B), as reported previously (Sawin et al., 1992) and consistent with data from other



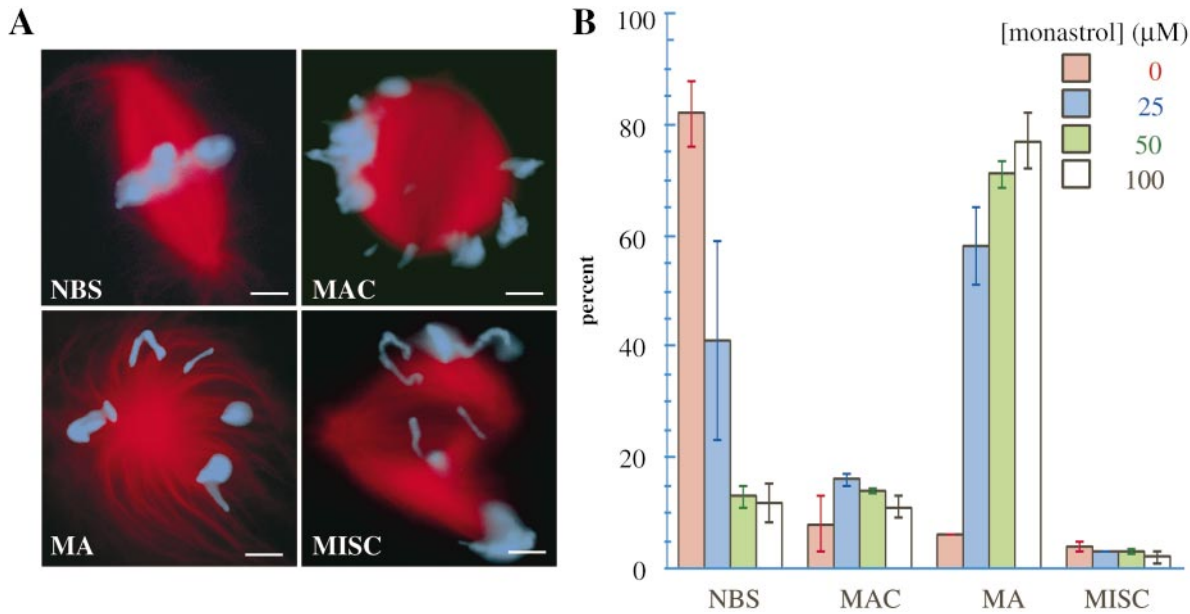


**Figure 7.** Monastrol inhibits the assembly of bipolar spindles in *Xenopus egg* extracts. Tetramethyl rhodamine–labeled tubulin and Hoechst 33342 were added to CSF-arrested *Xenopus egg* extracts to visualize the microtubules (red) and the chromatin (blue). Calcium was added to drive the extract into interphase after which monastrol and CSF-arrested extract were added. (A) The different structures observed around chromatin were categorized as normal bipolar spindles (NBS), spindles with misaligned chromosomes (MAC), monoasters (MA), and miscellaneous (MISC). (B) Monastrol inhibits the formation of bipolar spindles in a dose-dependent manner. The different structures observed in spindles assembled at different concentrations of monastrol are shown. Greater than 200 structures were counted in two independent experiments and the averages are shown ( $\pm$ SE). Bars: 5  $\mu$ m.

systems (Hagan and Yanagida, 1990; Blangy et al., 1995). In the presence of monastrol, Eg5 is still localized primarily at the poles of the now monoastrial spindle. Some punctate Eg5 staining is also observed along the microtubules in the monoasters (Fig. 8 D). It is difficult to quantitatively compare Eg5 localization in the bipolar and monoastrial spindles. In *in vitro* assays, monastrol inhibits the *Xenopus* Eg5-dependent microtubule gliding. Using microtubule pelleting assays, we find that monastrol does not inhibit the microtubule binding of recombinant Eg5 in high ATP and high salt (see Online Supplementary Material). Thus, microtubule binding and the localization of Eg5 at spindle poles are not sufficient for bipolar spindle formation and probably require the motility of the kinesin.

**Table III.** Statistics of Mad2 Localization at Kinetochores in Monastrol-treated Ptk2 Cells

Cell	Kinetochores detected	Mad2-positive kinetochores	Chromosomes with Mad2 staining one kinetochore	Chromosomes with Mad2 staining two kinetochores	Chromosomes with Mad2 staining no kinetochores
1	28	14	12	1	1
2	28	14	12	0	2
3	28	14	11	0	3
4	28	13	9	2	2
5	26	14	10	2	2
			78 ( $\pm$ 8)%	7 ( $\pm$ 7)%	15 ( $\pm$ 8)%

SD is in parentheses.

### Spindle Poles Stay Organized in the Presence of Monastrol

We next examined the organization of spindle poles in structures formed in *Xenopus egg* extracts treated with monastrol. NuMA is a structural protein that localizes to the spindle pole and interacts with the microtubule motor, dynein (Merdes et al., 1996). Fig. 9 A shows the localization of NuMA at the poles of a control spindle assembled in *Xenopus egg* extracts. Addition of 50  $\mu$ M monastrol at the start of the spindle assembly in cycled extracts leads to monoasters that have NuMA localized at their centers (Fig. 9 B), indicating that the microtubule minus ends are focused at the center of these structures. Concentrations of monastrol higher than 100  $\mu$ M result in asters with a cleared center (holey asters) (data not shown), reminiscent of structures observed in Eg5-specific antibody inhibition of aster formation in cell extracts (Sawin et al., 1992; Mountain et al., 1999).

We find that addition of monastrol to previously assembled bipolar spindles leads to their disassembly in *Xenopus egg* extracts. An image of a disassembling spindle fixed 20 min after monastrol addition to preformed spindles is shown in Fig. 9 C. The configuration of the microtubules and the chromatin correlates well with the real time imaging experiments described below. There is a remnant of the original bipolar spindle still present in this structure with NuMA localized to its poles. The NuMA staining and microtubule organization show the poles to be focused even at late stages of spindle disassembly. This indicates

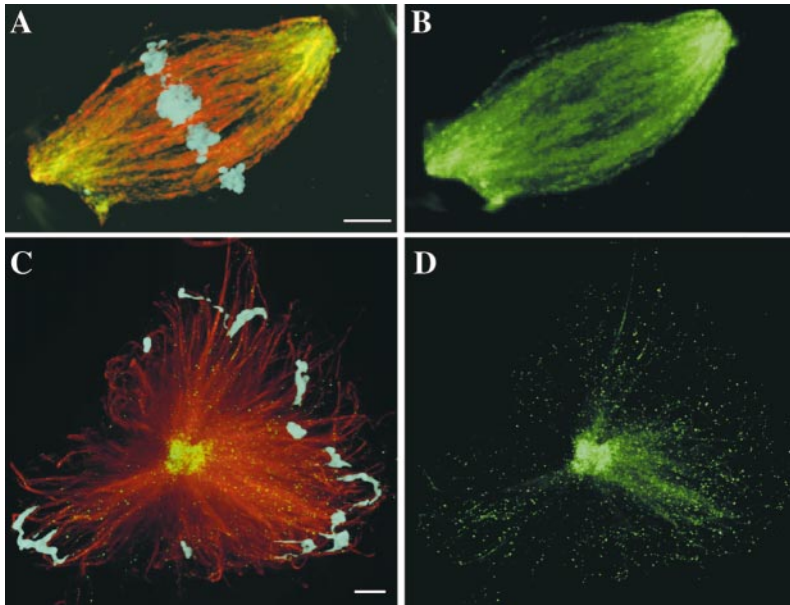


**Figure 8.** Immunolocalization of Eg5 in bipolar and monoastral spindles. At the completion of the cycled spindle assembly reaction, the spindles were diluted, fixed, layered over glycerol cushions, and spun onto coverslips. The samples were then processed for immunofluorescence. (A) An overlay shows the chromatin (blue), tubulin (red), and Eg5 (green) in a bipolar spindle assembled *in vitro*. (B) Eg5 alone. The protein is localized along microtubules and shows enrichment at the spindle poles. (C) Addition of 50  $\mu\text{M}$  monastrol to assembly reactions results in the formation of monoastral spindles. An overlay of the chromatin (blue), tubulin (red), and Eg5 (green) is shown. (D) Eg5 is immunolocalized along microtubules and is concentrated at the center of the monoaster. Bars: 5  $\mu\text{m}$ .

that monastrol concentrations that inhibit the formation of bipolar spindles in *Xenopus* egg extracts do not inhibit activities that maintain the localization of structural proteins at the poles and the focusing of the minus ends of the microtubules.

#### **Real Time Observations of Monastrol-induced Spindle Disassembly**

To examine the forces required for maintenance of bipolar spindles in *Xenopus* egg extracts, we imaged the effect of monastrol on preassembled bipolar spindles. Monastrol (50  $\mu\text{M}$ ) rapidly disassembles bipolar spindles assembled in *Xenopus* egg extracts. If spindles were trapped between a closely opposed coverslip and slide, the rate of disassembly was slower than that observed in test tubes or in thick sample preparations (see Materials and Methods and sup-

plemental video at <http://www.jcb.org/cgi/content/full/150/5/975/DC1>). Under imaging conditions that allowed spindle disassembly to proceed uninhibited by physical constraints, spindles moved around, requiring continuous adjustment of the focus and the X and Y coordinates of the microscope stage throughout the video. Fluorescently labeled tubulin and DNA staining dye were added to the extract to visualize the microtubules and chromatin. A montage of a representative time lapse video is shown in Fig. 10 A. It takes  $\sim 5$  min after mixing in the inhibitor to find and focus on a bipolar structure and acquire the first image. The video is 22.3 min in length.

In the earliest stages of the disassembly, the metaphase plate rapidly falls apart and chromosomes are ejected orthogonal to the pole-to-pole axis. Even in the first frame of the video, the chromatin at the metaphase plate is not as tightly centered within the spindle as in control spindles

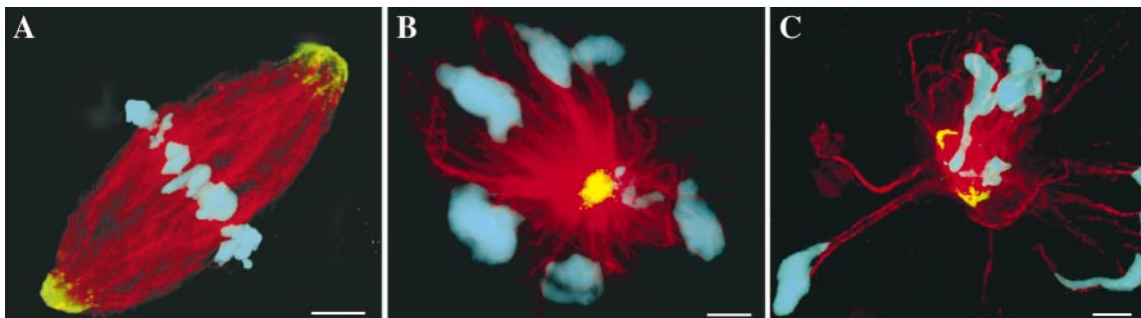


**Figure 9.** Monastrol concentrations that inhibit bipolar spindle formation do not disrupt the organization of spindle poles. Immunolocalization of NuMA was used to examine the organization of the minus ends of microtubules in structures assembled in *Xenopus* egg extracts. (A) An overlay shows the chromatin (blue), tubulin (red), and NuMA (green) in a bipolar spindle assembled in cycled extracts. (B) Addition of 50  $\mu\text{M}$  monastrol at the start of assembly reactions results in the formation of monoastral spindles. An overlay of the chromatin, tubulin, and NuMA shows NuMA, and thus microtubule minus ends, focused in the middle of the monoastral structure. (C) 50  $\mu\text{M}$  monastrol was added to a sample of preformed bipolar spindles and the sample was fixed after 20 min, corresponding to the time of significant disassembly (see Fig. 10). The overlay shows a disassembled bipolar spindle that has lost the chromatin from the metaphase plate but has a small bipolar unit with focused poles. NuMA is localized to the focused poles in all intermediates of spindle disassembly that we examined. Bars: 5  $\mu\text{m}$ .

A

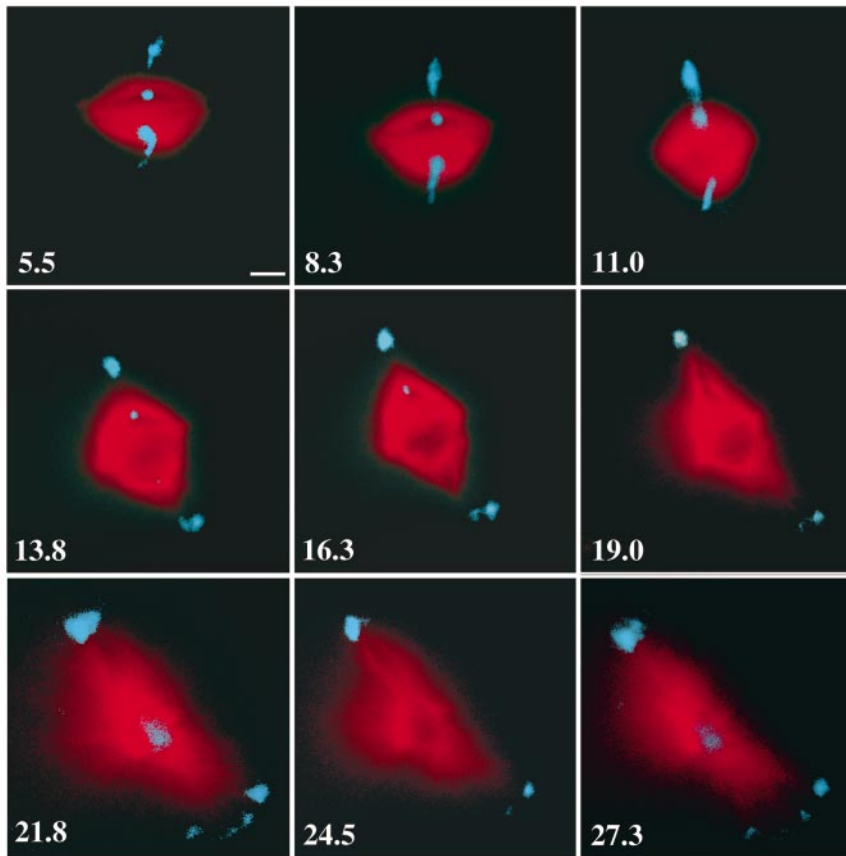
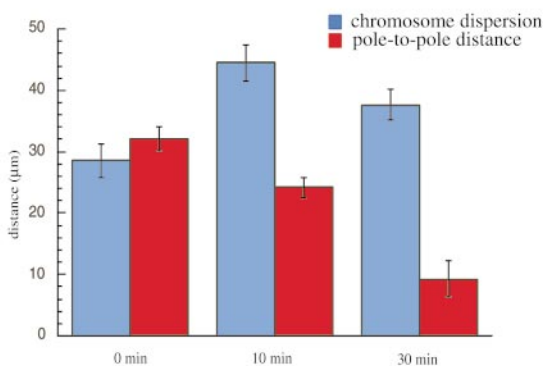


**Figure 10.** Monastrol-induced disassembly of preformed bipolar spindles. 50  $\mu\text{M}$  monastrol was added to bipolar spindles assembled in *Xenopus* egg extract and the sample was immediately prepared for imaging. The disassembling spindle moved in the sample, and the X, Y, and Z coordinates of the stage were adjusted through the course of the experiment. The time (min) after the addition of monastrol to the extract is indicated. Microtubules (red) and DNA (blue) are shown. (See supplemental video at <http://www.jcb.org/cgi/content/full/150/5/975/DC1>.) (B) At fixed time points, aliquots from disassembly reactions were removed and processed for imaging. Two parameters, the chromosome dispersion, defined as the diameter of the smallest circle enclosing all the chromosomes in a spindle, and the pole-to-pole distance were measured ( $n = 10$  for each time point). The increase in the chromosome index is completed by 10 min, while the reduction in pole-to-pole distance is only 35% complete. Bar: 5  $\mu\text{m}$ .

B



(see Figs. 7 A and 8 A). During the disassembly, spindle microtubules splay out of the spindle midzone, but remain attached to the spindle poles. Microtubule attachment to the chromatin is not lost at any time during the disassembly process. Significant reduction in the distance between poles is not discernible until  $\sim 11$  min after the addition of monastrol. After that, the poles slowly move together at an overall rate of  $\sim 1 \mu\text{m}/\text{min}$  until the structure becomes monoastrol. As observed for disassembling bipolar spindles at fixed time points (Fig. 9 C), the spindle poles stay focused through the disassembly process. Once the structures became radially symmetrical, no further major changes were observed. Control (untreated) bipolar spindles imaged for similar lengths of time under identical conditions did not show any loss of bipolarity or chromosome mislocalization.

During real time observations of monastrol-induced disassembly of bipolar spindles, we are unable to image the structure before or at the time of inhibitor addition. To compare the chromosome movements relative to the pole-to-pole distance, we took samples from disassembly reactions at fixed time points and measured two parameters, the pole-to-pole distance and the diameter of the smallest circle enclosing all chromosomes in a spindle (named chromosome dispersion) (Fig. 10 B). 10 min after the addition of monastrol to the sample, the chromosome dispersion increases to its maximum value while the reduction in the pole-to-pole distance is only 35% complete. The subsequent decrease in chromosome dispersion results from the decrease in the distance between the chromosome poles. Thus, inhibiting Eg5 motility by monastrol results in inactivation of the forces that keep microtubules cross-

linked at the spindle midzone, extrusion of chromosomes and attached microtubules out of the spindle, and spindle collapse by slow movements of the poles towards each other.

## Discussion

### *Monastrol Is a Reversible and Specific Probe for Eg5-dependent Mitotic Processes*

The usefulness of small molecules in cell biology depends on their specificity. We have examined the specificity of the inhibition of mitotic processes by monastrol in different ways. Unlike commonly used antimitotic agents such as nocodazole and taxol, monastrol does not affect the organization of microtubules in interphase cells or tubulin polymerization in vitro (Mayer et al., 1999). We have previously shown that monastrol does not disrupt lysosome and Golgi apparatus organization in interphase cells or chromosome dynamics in mitotic cells. We now show that monastrol does not inhibit S phase, G2 phase, or mitotic entry and that the reversal of the mitotic arrest due to monastrol is faster than the release of cells arrested by the microtubule poison, nocodazole. These fast kinetics of reversal should add to the usefulness of monastrol as a reagent for mitosis research in general.

Light and electron microscopy show that monastrol does not inhibit the centrosome duplication cycle. We have previously shown that monastrol inhibits the in vitro motility of Eg5, but does not inhibit conventional kinesin in vitro or other cellular processes dependent on other kinesin superfamily members (Mayer et al., 1999). Motor proteins such as dynein have been implicated in maintaining the localization of centrosomes and centrosomal proteins at spindle poles (Merdes et al., 1996; Mountain et al., 1999). Addition of monastrol to bipolar spindles assembled in vitro results in the formation of monoasters, but during the disassembly reaction, the spindle poles stay focused and organized, indicating that dynein- and pole-associated activities are not inhibited by monastrol. We have also examined several structural analogues of monastrol and find that every analogue that inhibits cells in mitosis with monoastrol spindles also inhibits Eg5 motility in vitro (Maliga, Z., T.M. Kapoor, T.U. Mayer, and T.J. Mitchison, manuscript in preparation). Together, these observations underscore the specificity of monastrol, a small molecule that arrests cells in mitosis by inhibiting the kinesin Eg5.

### *The Role of Eg5 in Spindle Assembly*

We have used monastrol to probe the function of Eg5 and its contribution to the organization and maintenance of the bipolar spindle assembled in *Xenopus* egg extracts. Our in vitro data (see Online Supplemental Material and Figure S1 at <http://www.jcb.org/cgi/content/full/150/5/975/DC1>) and observations suggest that monastrol inhibits Eg5 motility and not its microtubule binding. Also, monastrol does not prevent the localization of Eg5 to monoastrol spindles. Therefore, we can conclude that Eg5 localizes to spindles in part by mechanisms that do not require it to be an active motor. Furthermore, localization of Eg5 at spindle poles is not sufficient for bipolar spin-

dle formation and probably requires the motility of the kinesin.

Gheber et al. (1999) have compared mutants of Cin8, the *S. cerevisiae* homologue of Eg5, in vivo and in vitro. For cin8-3, the microtubule gliding was impaired but not the microtubule binding. However, this mutant was capable of generating bipolar spindles more efficiently than another mutant form, cin8-F467A, whose in vitro microtubule binding was compromised but not its motility. Based on these observations, the authors propose that the ability of the motor to bind microtubules is more important for establishing bipolar spindles than the motor's motility. The disparity between these observations in yeast and our data in *Xenopus* extracts is likely to represent differences between the spindles in these two systems. Alternatively, pole localization may not simply be a function of the microtubule binding sites on Eg5 but rather due to interactions with other proteins (Blangy et al., 1997).

Inhibition of Eg5 with monastrol reveals the existence of forces orthogonal to the spindle axis that rapidly extrude the chromosomes. Similar forces can be inferred during anaphase in *Xenopus* egg extracts, in which Murray et al. (1996) have observed the outward splaying of spindle microtubules when sister chromatids separate in bipolar spindles. What is the likely source of these forces orthogonal to the pole-to-pole axis in bipolar spindles? All previous discussions of forces in the spindle have focused on forces acting parallel to the microtubules. Even the "polar wind," a force that acts on chromosomes in the spindle, is discussed in this light (for review see Rieder and Salmon, 1994). However, Eg5 motility appears to be required to offset extrusive forces acting normal to the microtubule direction, in CSF-arrested bipolar spindles. This normal force could result from steric exclusion of large objects from the spindle, or from microtubule-microtubule repulsion operating at the spindle poles due to steric or cross-linking factors. We hypothesize that Eg5 offsets extrusive forces by cross-linking microtubules or delivering cross-linking activities to the middle of the spindle, working against microtubule polewards flux and dynamics.

Our data confirm that Eg5 is required for spindle pole separation at the onset of mitosis in somatic cells and in *Xenopus* extract spindles. However, our results are ambiguous on the role of Eg5 in the assembled bipolar spindle. Metaphase BS-C-1 cells treated with monastrol proceeded to anaphase without spindle disassembly, whereas extract spindles were rapidly disassembled. This latter observation has two possible explanations. Monastrol may enter the cells too slowly to destabilize the spindle before anaphase onset. We have no independent measure of the rate of cell entry of monastrol but we do know that cells with monoastrol spindles can be observed within 30 min of treatment. From washout experiments, it is clear that monastrol can equilibrate out of cells in minutes (see Fig. 1 D), suggesting that the compound may enter cells equally fast. Alternatively, Eg5 function may not be essential to maintain spindle bipolarity or its function may be masked by other activities that complete mitosis. Consistent with this explanation, Blangy et al. (1995) have shown that injection of Eg5-specific antibodies into HeLa cells that already have a bipolar spindle does not lead to spindle collapse or inhibit anaphase. Saunders and Hoyt (1992) have also shown that



in *S. cerevisiae*, deletion of Cin8 does not inhibit anaphase. Alternatively, the ongoing requirement for Eg5 may be system dependent. For example, in tissue culture cells, cortical dynein might help keep the poles apart once the spindle is built (Busson et al., 1998). While the generality of our observations in *Xenopus* egg extracts is not yet clear, we do think that these observations reveal a set of forces that act in spindles, whose significance is likely to be general.

### Detection and Correction of Syntelic Orientation

Using light and electron microscopy, we observed that many, perhaps most, of the chromosomes in monastrol-treated Ptk2 cells show syntelic orientation, with both kinetochores attached to the center of the monoasters, by parallel, calcium-stable kinetochore fibers. The ability of sister chromatids to adopt this orientation demonstrates a surprising flexibility in the linkage between sister kinetochores in Ptk cells. Syntelic orientation could result from collapse of a bipolar spindle, but our real time observations suggest that monastrol-treated cells entering mitosis gain this syntelic orientation by de novo capture of microtubules from a single pole by both kinetochores in a sister pair. We propose that the orientations of the chromosomes we have documented are a manifestation of the robust microtubule-kinetochore attachment possible in the presence of monastrol. By this argument, syntelic chromosome orientation is not observed in monoastrol structures such as "chromosome spheres," that form when centrosome separation is inhibited in Ptk1 cells treated with low concentrations of colcemid, a microtubule depolymerizer (for review see Rieder, 1982), because this agent either weakens the kinetochore-microtubule interactions or reduces the ability of microtubules to dynamically explore space and become captured by kinetochores (Rieder and Salmon, 1998).

Syntelic orientation is a common error early in meiotic spindles (Nicklas, 1971), but its prevalence in early mitosis is less clear. A systematic analysis of the frequency at which syntelic orientation of chromosomes occurs by spontaneous mistakes during mitosis has not been documented. Roos has described this form of chromosome malorientation as a rare event during prometaphase in Ptk cells (Roos, 1973; Roos, 1976; Rieder, 1982). In spontaneous monopolar spindles in newt cells, syntelic orientation of chromosomes has not been observed (Cassimeris, L., and E.D. Salmon, personal communication). However, Ault and Rieder (1992) propose that syntelic orientation of chromosomes is likely to be a common error in mitosis, and that a specific mechanism must exist for correcting it, as has been demonstrated in meiosis. However, it has been difficult to study syntelic orientation in mitosis because it is normally transient, and presumably rapidly corrected. In monastrol-treated cells, as many as 70% of the chromosomes can be syntelically oriented at steady state. Monastrol treatment may thus provide an experimental opportunity to study mechanisms by which syntelic orientation is detected and corrected. We suspect that the Mad2 staining we observe on one of the syntelic sister kinetochore pairs, typically the outer sister, may represent detection of the syntelic error. We do not yet know if error correction is at-

tempted in the presence of monastrol. Two mechanisms for correction of syntelic error have been proposed from meiotic studies, where the first event is the microtubule capture from the opposite pole (Church and Lin, 1985; Nicklas and Kubai, 1985) or microtubule release at the attached pole (Kitanishi-Yamura and Fukui, 1987; Ault and Nicklas, 1989). The former could not occur in continued monastrol treatment since only a single functional pole exists, though it would occur rapidly after washout. The latter, if it is a real mechanism, might occur continually in the monastrol-treated cell in a futile attempt to correct the error. In either case, monastrol will provide a tool to systematically study how syntelic orientation is corrected.

Our observations suggest that Mad2 localization at kinetochores cannot simply be a sensor for microtubule attachment. It is more likely that the Mad2 localization at kinetochores senses a subtler aspect of microtubule attachment, for example, the exact number of microtubules at the kinetochore or even the dynamic behavior of kinetochores. In some systems, tension at the kinetochore has been proposed to be an important signal for checkpoint activation (Nicklas et al., 1995; Nicklas, 1997). Monastrol-treated cells have condensed chromosomes that maintain dynamic attachments with microtubules. During oscillations, chromosomes in monoasters should experience forces that fluctuate and even change directions. It is likely that tension at either of these kinetochores would be variable. We anticipate that combining immunoelectron microscopy with a detailed analysis of microtubule number at different kinetochores will facilitate the characterization of the signal that regulates Mad2 localization to kinetochores. Correlating these observations with the dynamics of chromosomes in monastrol-treated cells should allow the mechanism of checkpoint activation to be clarified.

We thank E.D. Salmon, Y. Zheng, D.A. Compton, and C.E. Walczak for the antibodies and E.D. Salmon, C.L. Rieder, and members of the Mitchison laboratory for helpful discussions and comments on the manuscript. We thank P. Maddox, E.D. Salmon, and A. Desai for their assistance in imaging *Xenopus* extract preparations. T.M. Kapoor is a Runyon-Winchell Fellow. T.U. Mayer is a fellow of the Deutsche Forschungsgemeinschaft.

This work was also supported by grants from the Human Frontier Science Program and the National Institute of General Medical Sciences (39565).

Submitted: 18 May 2000

Revised: 17 July 2000

Accepted: 17 July 2000

### References

- Agard, D.A., Y. Hiraoka, P. Shaw, and J.W. Sedat. 1989. Fluorescence microscopy in three dimensions. *Methods Cell Biol.* 30:353-377.
- Ault, J.G., and R.B. Nicklas. 1989. Tension, microtubule rearrangements, and the proper distribution of chromosomes in mitosis. *Chromosoma.* 98:33-39.
- Ault, J.G., and C.L. Rieder. 1992. Chromosome mal-orientation and reorientation during mitosis. *Cell Motil. Cytoskeleton.* 22:155-159.
- Blangy, A., L. Arnaud, and E. Nigg. 1997. Phosphorylation by p34<sup>cdc2</sup> protein kinase regulates binding of the kinesin-related motor HsEg5 to the dynactin subunit p150<sup>glued</sup>. *J. Biol. Chem.* 272:19418-19424.
- Blangy, A., H. Lane, P. Herin, M. Harper, M. Kress, and E. Nigg. 1995. Phosphorylation by p34<sup>cdc2</sup> regulates spindle association of human Eg5, a kinesin-related motor essential for bipolar spindle formation in vivo. *Cell.* 83:1159-1169.
- Borisy, G.G., and E.W. Taylor. 1967. The mechanism of action of colchicine. Colchicine binding to sea urchin eggs and the mitotic apparatus. *J. Cell Biol.* 34:535-548.

- Busson, S., D. Dujardin, A. Moreau, J. Dompierre, and J.R. De Mey. 1998. Dynein and dynactin are localized to astral microtubules and at cortical sites in mitotic epithelial cells. *Curr. Biol.* 8:541–544.
- Chen, R.H., J.C. Waters, E.D. Salmon, and A.W. Murray. 1996. Association of spindle assembly checkpoint component XMAD2 with unattached kinetochores. *Science.* 274:242–246.
- Church, K., and H.P. Lin. 1985. Kinetochores microtubules and chromosome movement during prometaphase in *Drosophila melanogaster* spermatocytes studied in life and with the electron microscope. *Chromosoma.* 92:273–282.
- Cottingham, F.R., L. Gheber, D.L. Miller, and M.A. Hoyt. 1999. Novel roles for *Saccharomyces cerevisiae* mitotic spindle motors. *J. Cell Biol.* 147:335–350.
- Desai, A., A. Murray, T.J. Mitchison, and C.E. Walczak. 1999. The use of *Xenopus* egg extracts to study mitotic spindle assembly and function in vitro. *Methods Cell Biol.* 61:385–412.
- Enos, A.P., and N.R. Morris. 1990. Mutation of a gene that encodes a kinesin-like protein blocks nuclear division in *A. nidulans*. *Cell.* 60:1019–1027.
- Gheber, L., S.C. Kuo, and M.A. Hoyt. 1999. Motile properties of the kinesin-related Cin8p spindle motor extracted from *Saccharomyces cerevisiae* cells. *J. Biol. Chem.* 274:9564–9572.
- Hagan, I., and M. Yanagida. 1990. Novel potential mitotic motor protein encoded by the fission yeast *cut7+* gene. *Nature.* 347:563–566.
- Hagan, I., and M. Yanagida. 1992. Kinesin-related *cut7* protein associates with mitotic and meiotic spindles in fission yeast. *Nature.* 356:74–76.
- Heck, M.M., A. Pereira, P. Pesavento, Y. Yannoni, A.C. Spradling, and L.S. Goldstein. 1993. The kinesin-like protein KLP61F is essential for mitosis in *Drosophila*. *J. Cell Biol.* 123:665–679.
- Hildebrandt, E.R., and M.A. Hoyt. 2000. Mitotic motors in *Saccharomyces cerevisiae*. *Biochim. Biophys. Acta.* 1496:99–116.
- Hoyt, M.A., L. He, K.K. Loo, and W.S. Saunders. 1992. Two *Saccharomyces cerevisiae* kinesin-related gene products required for mitotic spindle assembly. *J. Cell Biol.* 118:109–120.
- Hoyt, M.A., L. Totis, and B.T. Roberts. 1991. *S. cerevisiae* genes required for cell cycle arrest in response to loss of microtubule function. *Cell.* 66:507–517.
- Hyman, A., D. Drechsel, D. Kellogg, S. Salsler, K. Sawin, P. Steffen, L. Wordeman, and T. Mitchison. 1991. Preparation of modified tubulins. *Methods Enzymol.* 196:478–485.
- Inoue, S., and E.D. Salmon. 1995. Force generation by microtubule assembly/disassembly in mitosis and related movements. *Mol. Biol. Cell.* 6:1619–1640.
- Khodjakov, A., R.W. Cole, B.R. Oakley, and C.L. Rieder. 2000. Centrosome-independent mitotic spindle formation in vertebrates. *Curr. Biol.* 10:59–67.
- Kitanishi-Yamura, T., and Y. Fukui. 1987. Reorganization of microtubules during mitosis in *Dictyostelium*: dissociation from MTOC and selective assembly/disassembly in situ. *Cell Motil. Cytoskeleton.* 8:106–117.
- Li, R., and A.W. Murray. 1991. Feedback control of mitosis in budding yeast [published erratum at 79:following 388]. *Cell.* 66:519–531.
- Li, Y., and R. Benezra. 1996. Identification of a human mitotic checkpoint gene: *hMAD2*. *Science.* 274:246–248.
- Mayer, T.U., T.M. Kapoor, S.J. Haggarty, R.W. King, S.L. Schreiber, and T.J. Mitchison. 1999. Small molecule inhibitor of mitotic spindle bipolarity identified in a phenotype-based screen. *Science.* 286:971–974.
- Merdes, A., K. Ramyar, J.D. Vechio, and D.W. Cleveland. 1996. A complex of NuMA and cytoplasmic dynein is essential for mitotic spindle assembly. *Cell.* 87:447–458.
- Mitchison, T. 1989. Polewards microtubule flux in the mitotic spindle: evidence from photoactivation of fluorescence. *J. Cell Biol.* 109:637–652.
- Mitchison, T., L. Evans, E. Schulze, and M. Kirschner. 1986. Sites of microtubule assembly and disassembly in the mitotic spindle. *Cell.* 45:515–527.
- Mitchison, T.J. 1994. Towards a pharmacological genetics. *Chem. Biol.* 1:3–6.
- Mountain, V., C. Simerly, L. Howard, A. Ando, G. Schatten, and D.A. Compton. 1999. The kinesin-related protein, HSET, opposes the activity of Eg5 and cross-links microtubules in the mammalian mitotic spindle. *J. Cell Biol.* 147:351–366.
- Murray, A.W., A.B. Desai, and E.D. Salmon. 1996. Real time observation of anaphase in vitro. *Proc. Natl. Acad. Sci. USA.* 93:12327–12332.
- Nicklas, R.B. 1971. Mitosis. *Adv. Cell Biol.* 2:225–297.
- Nicklas, R.B. 1997. How cells get the right chromosomes. *Science.* 275:632–637.
- Nicklas, R.B., and D.F. Kubai. 1985. Microtubules, chromosome movement, and reorientation after chromosomes are detached from the spindle by micromanipulation. *Chromosoma.* 92:313–324.
- Nicklas, R.B., S.C. Ward, and G.J. Gorbsky. 1995. Kinetochores chemistry is sensitive to tension and may link mitotic forces to a cell cycle checkpoint. *J. Cell Biol.* 130:929–939.
- Rieder, C.L. 1982. The formation, structure, and composition of the mammalian kinetochores and kinetochores fiber. *Int. Rev. Cytol.* 79:1–58.
- Rieder, C.L., and R.E. Palazzo. 1992. Colcemid and the mitotic cycle. *J. Cell Sci.* 102:387–392.
- Rieder, C.L., and E.D. Salmon. 1994. Motile kinetochores and polar ejection forces dictate chromosome position on the vertebrate mitotic spindle. *J. Cell Biol.* 124:223–233.
- Rieder, C.L., and E.D. Salmon. 1998. The vertebrate cell kinetochores and its roles during mitosis. *Trends Cell Biol.* 8:310–318.
- Roof, D.M., P.B. Meluh, and M.D. Rose. 1992. Kinesin-related proteins required for assembly of the mitotic spindle. *J. Cell Biol.* 118:95–108.
- Roos, U.P. 1973. Light and electron microscopy of rat kangaroo cells in mitosis. II. Kinetochores structure and function. *Chromosoma.* 41:195–220.
- Roos, U.P. 1976. Light and electron microscopy of rat kangaroo cells in mitosis. III. Patterns of chromosome behavior during prometaphase. *Chromosoma.* 54:363–385.
- Saunders, W.S., and M.A. Hoyt. 1992. Kinesin-related proteins required for structural integrity of the mitotic spindle. *Cell.* 70:451–458.
- Sawin, K., and T. Mitchison. 1991. Poleward microtubule flux mitotic spindles assembled in vitro. *J. Cell Biol.* 112:941–954.
- Sawin, K.E., K. LeGuellec, M. Philippe, and T.J. Mitchison. 1992. Mitotic spindle organization by a plus-end-directed microtubule motor. *Nature.* 359:540–543.
- Sharp, D.J., K.R. Yu, J.C. Sisson, W. Sullivan, and J.M. Scholey. 1999. Antagonistic microtubule-sliding motors position mitotic centrosomes in *Drosophila* early embryos. *Nature Cell Biol.* 1:51–54.
- Shelanski, M.L., and E.W. Taylor. 1967. Isolation of a protein subunit from microtubules. *J. Cell Biol.* 34:549–554.
- Sluder, G., F.J. Miller, and C.L. Rieder. 1989. Reproductive capacity of sea urchin centrosomes without centrioles. *Cell Motil. Cytoskeleton.* 13:264–273.
- Taylor, S.S., and F. McKeon. 1997. Kinetochores localization of murine Bub1 is required for normal mitotic timing and checkpoint response to spindle damage. *Cell.* 89:727–735.
- Walczak, C.E., I. Vernos, T.J. Mitchison, E. Karsenti, and R. Heald. 1998. A model for the proposed roles of different microtubule-based motor proteins in establishing spindle bipolarity. *Curr. Biol.* 8:903–913.
- Waters, J.C., R.H. Chen, A.W. Murray, and E.D. Salmon. 1998. Localization of Mad2 to kinetochores depends on microtubule attachment, not tension. *J. Cell Biol.* 141:1181–1191.
- Winey, M., L. Goetsch, P. Baum, and B. Byers. 1991. MPS1 and MPS2: novel yeast genes defining distinct steps of spindle pole body duplication. *J. Cell Biol.* 114:745–754.